Zeitschrift: IABSE proceedings = Mémoires AIPC = IVBH Abhandlungen
Band: 5 (1981)
Heft: P-48: Numerical analysis of continuous helicoidal girders

Artikel: Numerical analysis of continuous helicoidal girders
Autor: Pulmano, V.A. / Kabaila, A.P.
DOI: https://doi.org/10.5169/seals-35892

Numerical Analysis of Continuous Helicoidal Girders

Calcul numérique de poutres continues spirales

Numerische Berechnung durchlaufender spiralförmiger Träger

V.A. PULMANO Associate Professor

A.P. KABAILA Associate Professor

University of New South Wales
Kensington, Sydney, Australia

SUMMARY

A numerical analysis of continuous helicoidal girder by the stiffness method is presented. The full stiffness matrix of a helicoidal member is derived by first evaluating the flexibility matrix at one end which when inverted gives the end stiffness matrix. The integrals associated with the end flexibility matrix and equivalent load vector, are numerically evaluated by Simpson's rule using the computer. The analysis of a helicoidal girder of varying cross-section can easily be treated. Numerical examples are presented to illustrate the proposed method.

RÉSUMÉ

Une méthode numérique pour le calcul de poutres continues spirales est présentée. La matrice complète de rigidité d'un élément spiral est dérivée en évaluant la matrice de flexibilité à une extrémité puis en déterminant la matrice inverse. L'intégrale correspondant à la matrice de flexibilité et au vecteur charge est calculée numériquement à l'aide de la méthode de Simpson. Le calcul de poutres spirales à section variable est également possible. Des exemples numériques illustrent la méthode.

ZUSAMMENFASSUNG

Eine numerische Methode zur Berechnung durchlaufender spiralförmiger Träger wird dargestellt. Die vollständige Steifigkeitsmatrix eines spiralförmigen Elementes ergibt sich durch zahlenmässige Festlegung der Flexibilitätsmatrix an einem Ende und anschliessender Bestimmung der Kehrmatrix. Die der Flexibilitätsmatrix und dem äquivalenten Lastvektor zugeordneten Integrale werden zahlenmässig mittels Simpsonmethode festgelegt. Variable Querschnitte sind einfach zu berücksichtigen. Numerische Beispiele erläutern die vorgeschlagene Berechnungsmethode.

1. INTRODUCTION

Earlier works on helicoidal girders [1,2,3,4] treated mainly the problem of helicoidal staircases which are indeterminate to the sixth degree. The analysis of continuous helicoidal girder has been attempted by Abdul-Baki and Shukair [5] by deriving explicitly the end flexibility matrix of a helicoidal segment which, when inverted, gives the end stiffness matrix. However, the resulting expressions for the different terms in the end flexibility matrix are very lengthy, and therefore inconvenient. Derron and Jirousek [6] presented a method of analysis of helicoidal girders, which was based on an assumed displacement field. In this respect their analysis is similar to the customary finite element formulation leading to approximate solution. The accuracy of solution usually improves as the number of elements to model a given problem is increased.

In this paper the integrals associated with the derivation of the basic matrices, viz., flexibility matrix, equivalent nodal loads are derived in the exact form, but the integration is carried out numerically. The method, therefore, is substantially different from those described in the above references. The effects of bending, shear, axial and torsional deformations are included without difficulty, however the effects of warping are excluded. In the analysis, the structure is assumed to be linearly elastic, and to obey other basic assumptions related to small deflection theory. Numerical examples are presented.

2. THEORETICAL CONSIDERATIONS

2.1 Geometry and Axis Transformation

In Fig. 1(a), a helicoidal member AB is shown with the nodal coordinates in the positive directions and their numbering. The nodal axes are taken parallel to the orthogonal reference axes x_j. At any section C, defined by angle β, the member axes are defined by three mutually perpendicular axes $\bar{x}_1$, $\bar{x}_2$, and $\bar{x}_3$ which coincide respectively with the tangent to the helix, normal to the helix (which is also normal to the generator of the cylinder), and the binormal to the helix. The $\bar{x}_2$ and $\bar{x}_3$ axes are assumed to coincide with principal axes of the cross-section of the helicoidal member.

The member axis $\bar{x}_i$ and the reference axis x_j are related by the equations

$$\{\bar{x}\} = \begin{bmatrix} \ell_{11} & \ell_{12} & \ell_{13} \\ \ell_{21} & \ell_{22} & \ell_{23} \\ \ell_{31} & \ell_{32} & \ell_{33} \end{bmatrix} \{x\} = [\lambda]\{x\} \qquad (1)$$

in which $[\lambda]$ is the rotation matrix. The term ℓ_{ij} in Eq. 1 is the cosine of the angle between the member axis $\bar{x}_i$ and the reference axis x_j. Considering the geometry of the helicoidal member of Fig. 1, it can be shown that the terms of the rotation matrix, λ, are as follows:

$$[\lambda] = \begin{bmatrix} \cos\alpha\cos\beta & \cos\alpha\sin\beta & \sin\alpha \\ -\sin\beta & \cos\beta & 0 \\ -\sin\alpha\cos\beta & -\sin\alpha\sin\beta & \cos\alpha \end{bmatrix} \qquad (2)$$

Angle α defines the inclination of the helix, angle β, the position of the point considered. Both α and β are shown in Fig. 1.

2.2 End Flexibility of Helicoidal Member.

As shown in Fig. 1(b), end A of the helicoidal member AB is considered to be fixed. The end actions p_B, applied at B, are expressed in terms of the nodal axes. The internal actions, $\{\sigma_C\}$ at any section C are in terms of end actions p_B and are given by the matrix expression

$$\{\sigma_C\} = H \{p_B\} \tag{3}$$

in which $\{\sigma_C\} = \{N \quad S_{x_2} \quad S_{x_3} \quad T \quad M_{x_2} \quad M_{x_3}\}$, $\{p_B\} = \{p_{B_1} \; p_{B_2} \; p_{B_3} \; p_{B_4} \; p_{B_5} \; p_{B_6}\}$, H = transformation matrix, N = axial force, $S_{\bar{x}_2}$, $S_{\bar{x}_3}$ = shear forces in the $\bar{x}_2$ $\bar{x}_3$ directions, respectively, T = twisting moment, and $M_{\bar{x}_2}$, $M_{\bar{x}_3}$ = bending moments about $\bar{x}_2$ and $\bar{x}_3$ axes, respectively.

In Eq. 3, the transformation matrix H, as shown elsewhere [7], is simply the product of the rotation matrix, $\hat{R}$ and the translation matrix $\hat{T}$, that is,

$$H = \hat{R}\,\hat{T} \tag{4}$$

in which

$$\hat{R} = \begin{bmatrix} \lambda & 0 \\ 0 & \lambda \end{bmatrix} \quad (5) \qquad \hat{T} = \begin{bmatrix} I & 0 \\ \hat{X} & I \end{bmatrix} \quad (6) \qquad \hat{X} = \begin{bmatrix} 0 & -r_3 & r_2 \\ r_3 & 0 & -r_1 \\ -r_2 & r_1 & 0 \end{bmatrix} \tag{7}$$

$$r_1 = x_1^B - x_1^C = R(\sin \Omega_B - \sin \beta)$$
$$r_2 = x_2^B - x_2^C = R(-\cos \Omega_B + \cos \beta)$$
$$r_3 = x_3^B - x_3^C = R \tan \alpha \, (\Omega_B - \beta)$$

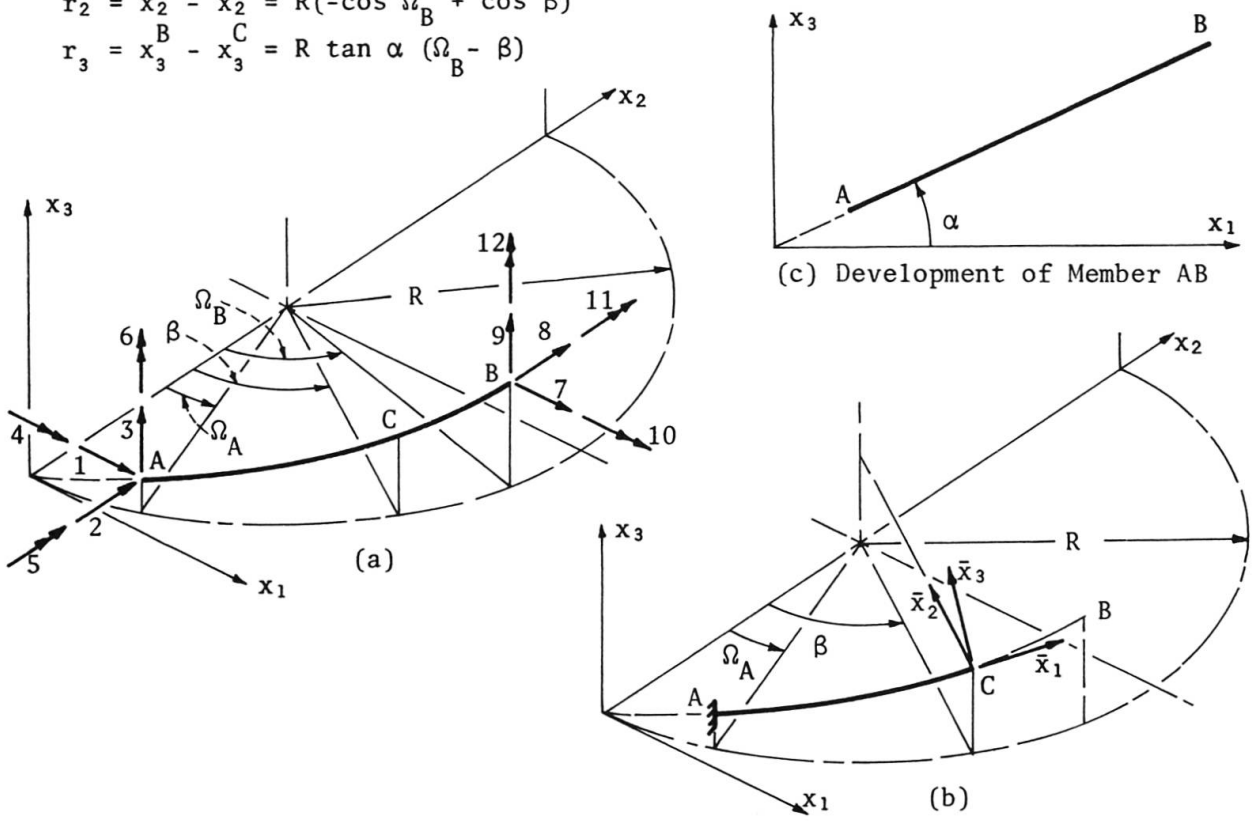

FIG. 1 HELICOIDAL MEMBER AB SHOWING ITS REFERENCE AXES, MEMBER AXES AND NUMBERING OF NODAL COORDINATES.

R = radius of circular cylinder defining the helix

I = (3x3) identity matrix

Substitution of Eqs. 5 and 6 to Eq. 4 yields

$$H = \begin{bmatrix} \lambda & 0 \\ \hat{\lambda X} & \lambda \end{bmatrix} \tag{8}$$

Using the principle of virtual work, the end flexibility, f_{BB}, of the helicoidal member AB is evaluated from the equation

$$f_{BB} = \int_A^B H^T D^{-1} H \, ds \tag{9}$$

where $D = \lfloor EA_1 \; GA_2 \; GA_3 \; GJ \; EI_2 \; EI_3 \rceil$, in which the symbol $\lfloor \rceil$ denotes a diagonal matrix

E = modulus of elasticity

A_1, A_2, A_3 = the area of section, the shear area in $\bar{x}_2$ - direction, and the shear area in $\bar{x}_3$ direction, respectively.

J = torsion constant

I_2, I_3 = moment of inertia about $\bar{x}_2$ and $\bar{x}_3$ axes, respectively

$ds = R \, d\beta / \cos \alpha$

In evaluating Eq. 9, a numerical procedure is used. This approach entails the evaluation of the various matrices at discrete points along the member and the integration is performed numerically by Simpson's rule.

2.3 Stiffness Matrix of Member AB

The inversion of matrix f_{BB} defined by Eq. 9 gives the end stiffness k_{BB}, i.e.

$$k_{BB} = f_{BB}^{-1} \tag{10}$$

such that

$$\{p_B\} = [k_{BB}] \{\bar{u}_B\} \tag{11}$$

in which $\{p_B\}$ and $\{u_B\}$ are the forces and displacements at the end of the cantilevered helicoidal member. If the helicoidal member is a part of a structure, then in addition to the displacements of one end relative to the other, it may also undergo rigid body motion defined by the displacement u_A at end A. In order to establish a member stiffness, k, these rigid body displacements must be taken into account. The stiffness matrix, k, which relates the end forces and end displacements in terms of nodal axes is given by the following equation,

$$\{p_A \; p_B\} = [k] \; \{u_A \; u_B\} \tag{12}$$

The end forces p_A at A are in equilibrium with p_B, thus

$$p_A = -\hat{T}\, p_B \tag{13}$$

The end actions at A and B in terms of the p_B are therefore given by

$$\begin{bmatrix} p_A \\ p_B \end{bmatrix} = \begin{bmatrix} -\hat{T} \\ I \end{bmatrix} [p_B] \tag{14}$$

and by contragredience,

$$[\bar{u}_B] = [-\hat{T}^T \; I] \{u_A \; u_B\} \tag{15}$$

Since the strain energy, U, in the helicoidal member remains the same with or without the inclusion of the rigid body motion, the strain energy in terms of k_{BB} is given by

$$U = \tfrac{1}{2}\, \bar{u}_B^T\, k_{BB}\, \bar{u}_B$$

$$= \tfrac{1}{2}[u_A^T \; u_B^T] \begin{bmatrix} -\hat{T} \\ I \end{bmatrix} [k_{BB}] [-\hat{T}^T \; I] \begin{bmatrix} u_A \\ u_B \end{bmatrix} \tag{16}$$

and in terms of the full stiffness matrix, k, of helicoidal member,

$$U = \tfrac{1}{2}[u_A^T \; u_B^T] \; [k] \begin{bmatrix} u_A \\ u_B \end{bmatrix} \tag{17}$$

Comparing Eqs. 16 and 17, it follows that

$$k = \begin{bmatrix} -\hat{T} \\ I \end{bmatrix} [k_{BB}] \; [-\hat{T}^T \; I] \tag{18}$$

or

$$k = \begin{bmatrix} \hat{T}\, k_{BB}\, \hat{T}^T & -\hat{T}\, k_{BB} \\ -k_{BB}\, \hat{T}^T & k_{BB} \end{bmatrix} \tag{19}$$

Equation 19 is the stiffness matrix of the helicoidal member AB expressed in terms of the nodal axes.

2.4 Equivalent Nodal Loads {Q}

2.4.1 Concentrated load on AB

Let the load vector at D, expressed in terms of the nodal axes, be denoted $\{p_D\} = \{ p_{D_1} \; p_{D_2} \; p_D \; \cdots \; p_{D_6} \}$. The angle Ω_D defines the location of load p_D as shown in Fig. 2(a). It can be shown that the displacement vector at the release B, caused by p_D at point D, is given by

$$u_{BO} = \int H^T\, D^{-1}\, H_o \, ds \tag{20}$$

where H_o is the transformation matrix of the loads at D to the internal actions $\{\sigma_C\}$. To calculate H_o, the expression given by Eq. 8 applies, but Ω_D replaces Ω_B, coordinates of point D replace that of B, and for $\beta > \Omega_D$, $H_o = 0$.

Having found u_{BO} and f_{BB}, the reaction p_B are found considering the compatibility condition,

$$u_{BO} + f_{BB}\, p_B = 0 \tag{21}$$

or

$$p_B = -f_{BB}^{-1}\, u_{BO} = -k_{BB}\, u_{BO} \tag{22}$$

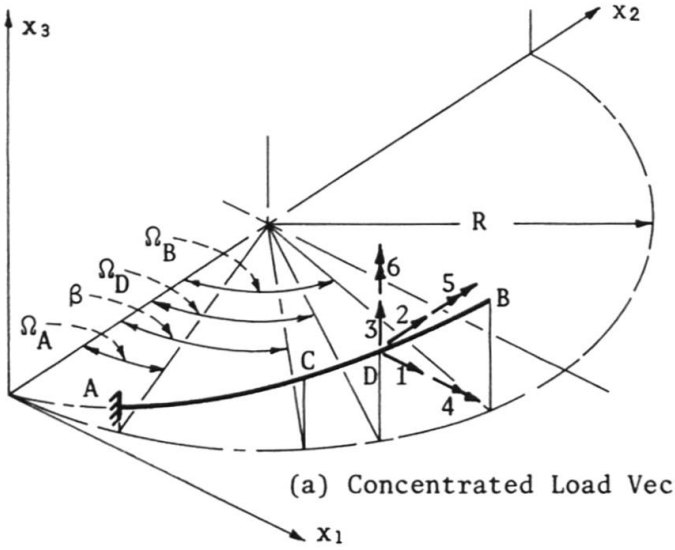

(a) Concentrated Load Vector at D, $\{p_D\}$

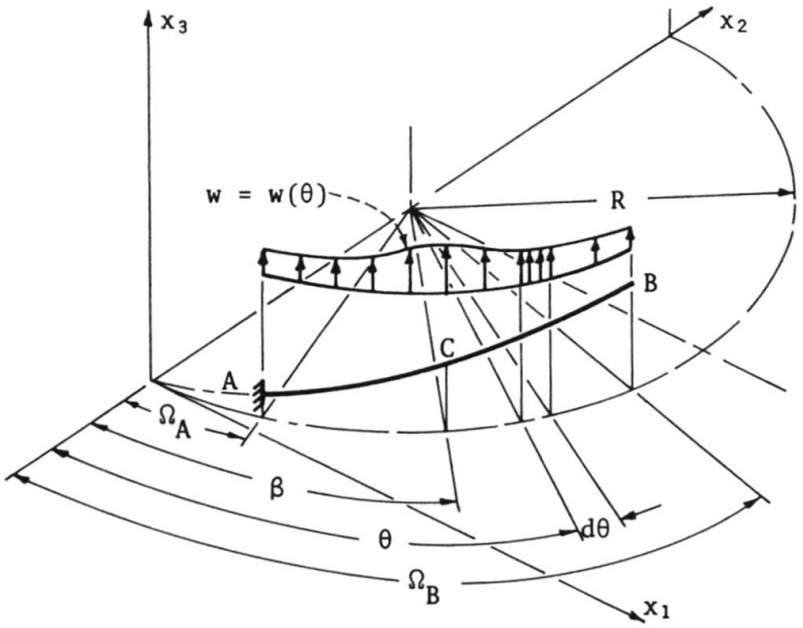

(b) Distributed Loading, $w = w(\theta)$

FIG. 2 CONCENTRATED AND DISTRIBUTED LOADINGS ON HELICOIDAL MEMBER AB.

By statics, the reactions at A are given by

$$p_A = -\hat{T}_{DA}\, p_D - \hat{T}_{BA}\, p_B \tag{23}$$

The equivalent nodal loads, $\{Q\} = \{Q_A\ Q_B\}$ which are numerically equal to the end reactions but act in the opposite directions, are given by,

$$\{Q\} = \{Q_A\ Q_B\} = -\{p_A\ p_B\} \tag{24}$$

2.4.2 Distributed Loading on AB

Consider the cantilevered helicoidal member AB subjected to a distributed loading, $w = w(\theta)$, in which θ is a horizontal angle as shown in Fig. 2(b). The components of the distributed loading are considered positive in the positive directions of the x_i - axes. The internal forces at any section C, due to distributed loading on portion CB, are given by

$$\{\sigma_C\} = \hat{R} \int_{\Omega_B}^{\beta} \hat{T}\, dF \tag{25}$$

where $\hat{R}$ and $\hat{T}$ are the rotation and translation matrices, respectively, and dF is the elemental load vector defined by angle θ.

For a uniformly distributed load with intensity w_o per unit length of the horizontal projection, and acting parallel to the x_3 - axis,

$$\{dF\} = \{0 \quad 0 \quad w_o R\, d\theta \quad 0 \quad 0 \quad 0\} \tag{26}$$

Substitution of Eq. 26 into Eq. 25, and evaluation of the resulting integral yields,

$$\{\sigma_c\} = \begin{bmatrix} \lambda & o \\ o & \lambda \end{bmatrix} \begin{bmatrix} 0 \\ 0 \\ w_o R\,(\beta-\Omega_B) \\ -w_o R^2\,[\sin\beta - \sin\Omega_B - (\beta-\Omega_B)\cos\beta] \\ +w_o R^2\,[\cos\beta - \cos\Omega_B + (\beta-\Omega_B)\sin\beta] \\ 0 \end{bmatrix} \equiv H_w \tag{27}$$

The end displacements u_{BO} due to a uniformly distributed load w_o is then given by,

$$u_{BO} = \int_{\Omega_A}^{\Omega_B} H\, D^{-1}\, H_w^T\, ds \tag{28}$$

and hence, the end reactions at B are

$$p_B = -k_{BB}\, u_{BO} \tag{29}$$

From equilibrium conditions, the reactions at A are

$$p_A = -\hat{T}_{BA}\, p_B - \int_{\Omega_B}^{\Omega_A} \hat{T}_{CA}\, dF \tag{30}$$

The second term of the right-hand side of Eq. 30 is simply equal to second matrix of the right-hand side of Eq. 27 but β is now replaced by Ω_A.

3. NUMERICAL EXAMPLES

3.1 Example 1 Deflections at Free End of Cantilever Helicoidal Girders

The vertical deflections at the free end of cantilevered helicoidal girders have been evaluated for girders with a uniform cross-section, linearly varying depth and parabolically varying depth. The geometric and material properties of these girders are given in the figure of Table 1.

The girder of a uniform section has been analysed considering two load cases, namely; (a) a point load at free end, and (b) a uniformly distributed load of intensity w_o per unit length of horizontal projection acting on the whole girder. Analyses were made with different values of the inclination angle, α, and the number of segments, n, which sub-divide the girder. The numerical results tabulated in Table 1 are in excellent agreement with the closed form solutions presented by Gerstle [8] . Note that Gerstle's solutions included only the effects of bending and torsional deformations. This accounts partially for the small differences between the two solutions.

The treatment of helicoidal girders of varying cross-section is easily done, and to illustrate this point two cantilever helicoidal girders, subjected to a point load at free end, were analysed. One is a girder with linearly varying depth, and the other, with a parabolically varying depth. Both girders have constant width. Numerical results for $\alpha = 15^o$ and $n = 32$ are given in Table 1.

3.2 Example 2 Fixed End Actions in Helicoidal Girders

A helicoidal girder of uniform section is analysed for equivalent nodal loads of two load cases, namely: (a) a point load at the midpoint of the girder, and (b) a uniformly distributed load of intensity w_o per unit length of horizontal projection, acting on the whole girder. Using 32 segments to sub-divide the girder, numerical values for equivalent nodal loads of each load case were obtained for two values of the inclination angle, $\alpha = 0^o$ and $\alpha = 20^o$, and are summarized in Table 2.

3.3 Example 3 Two-Span Helicoidal Girder

A continuous helicoidal girder consisting of two spans,as shown in the figure of Table 3, is fixed at the two ends, and supported at the midspan. The intermediate support prevents displacement in the vertical direction only. The girder was analysed for three load cases, namely: (a) a point load at midpoint of span AB only; (b) a uniformly distributed load of intensity w_o per unit length of horizontal projection acting on span BC only; and (c) load cases (a) and (b) combined. Numerical values for reactions at supports were obtained for two values of the inclination angle, $\alpha = 0^o$, and $\alpha = 20^o$, and are tabulated in Table 3. Note that the numerical results obtained for load case (c) are equal to the super-position of results obtained for load cases (a) and (b). This serves as a partial check to the solution.

4. CONCLUSIONS

In this paper a numerical procedure for the analysis of continuous helicoidal girder by the stiffness method is presented. The full stiffness matrix of a

TABLE 1 VERTICAL DEFLECTION COMPONENTS (mm) AT FREE END OF CANTILEVERED HELICOIDAL GIRDERS (EXAMPLE 1)

Load	No. of Segments n	Inclination Angle, α		
		0^o	15^o	30^o
Point Load		Girder with Uniform Section		
	8	-36.38673	-37.80223	-42.56490
	16	-36.38673	-37.80223	-42.56490
	Ref.[8]	-36.319	-37.750	-40.406
u.d.1	16	-9.69262	-10.06906	-11.33578
	Ref.[8]	-9.638	-	-
Point Load		Girder with Linearly Varying Depth		
	32	-	-15.99359	-
		Girder with Parabolically Varying Depth		
	32	-	-17.16251	-

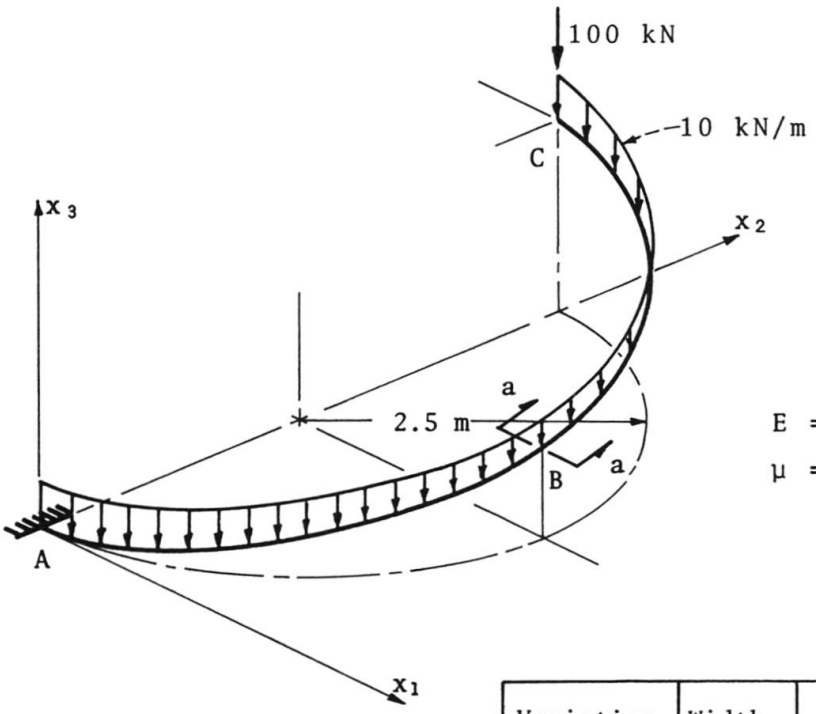

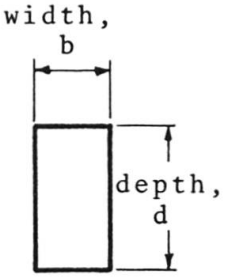

Section a-a

$E = 200 \times 10^6$ kPa

$\mu = 0.3$

Variation of depth	Width, b (mm)	Depth, d (mm)		
		d_A	d_B	d_C
Uniform	50	100	100	100
Linear		200	150	100
Parabolic		200	125	100

TABLE 2 EQUIVALENT NODAL LOADS FOR A POINT LOAD AND A UNIFORMLY DISTRIBUTED LOAD ON A HELICOIDAL MEMBER FOR VARIOUS VALUES OF THE INCLINATION ANGLE, α (EXAMPLE 2).

EQF Components	Inclination Angle, α		
	0^o	10^o	20^o
	Point Load, P = -100 kN, at B		
1	0.	-2.18725	-4.30213
2 } kN	0.	0.00014	0.00028
3	-50.00009	-50.00005	-49.99996
4	-45.42277	-45.09989	-44.12459
5 } kN-m	125.00030	123.48570	118.85100
6	0.	5.46836	10.75576
7	0.	2.18725	4.30213
8 } kN	0.	-0.00014	-0.00028
9	-49.99991	-49.99995	-50.00004
10	45.42233	45.09942	44.12400
11 } kN-m	124.99970	123.48530	118.85090
12	0.	5.46790	10.75487
	Uniformly distributed load (udl), w_o = -10 kN/m over whole span		
1	0.	-0.86175	-1.69479
2 } kN	0.	-0.00000	-0.00000
3	-39.26991	-39.26991	-39.26991
4	-18.59739	-18.47017	-18.08595
5 } kN-m	62.50000	61.90330	60.07763
6	0.	2.15438	4.23697
7	0.	0.86175	1.69479
8 } kN	0.	0.00000	0.00000
9	-39.26991	-39.26991	-39.26991
10	18.59739	18.47017	18.08595
11 } kN-m	62.50000	61.90330	60.07763
12	0.	2.15438	4.23697

EQF = equivalent nodal force

E = 200 x 10^6 kPa

μ = 0.3

b = 50 mm; d = 100 mm

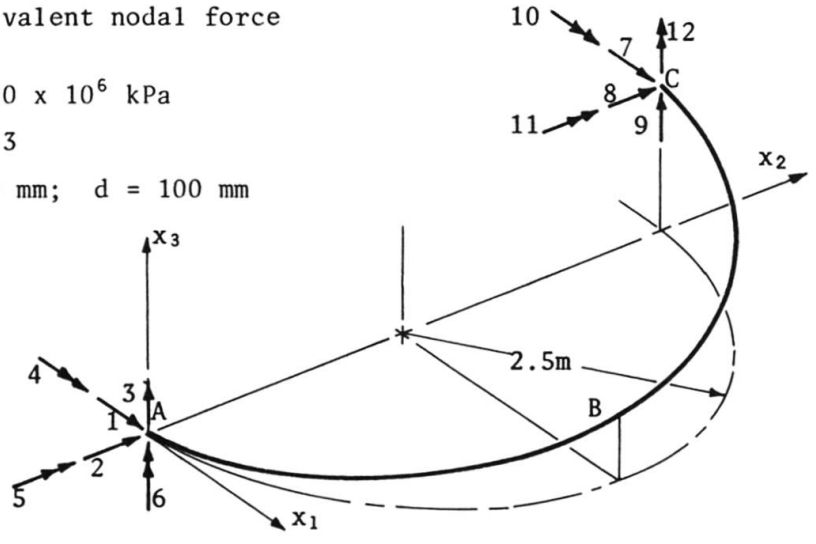

TABLE 3 REACTION COMPONENTS AT THE SUPPORTS OF A TWO-SPAN HELICOIDAL GIRDER (EXAMPLE 3).

Reaction Components	Only span AB Loaded	Only Span BC Loaded	Both Spans AB and BC Loaded
	Inclination Angle, $\alpha = 0^o$		
1	0.	0.	0.
2 kN	0.	0.	0.
3	64.48747	- 5.84984	58.63763
4	9.55895	- 1.53322	8.02573
5 kN-m	-80.45739	10.53136	-69.92603
6	0.	0.	0.
7	0.	0.	0.
8 kN	0.	0.	0.
9	-11.22502	46.47837	35.25335
10	2.94558	- 4.28729	- 1.34170
11 kN-m	20.52457	-40.75315	-20.22858
12	0.	0.	0.
13 kN	46.73755	37.91129	84.64884
	Inclination Angle, $\alpha = 20^o$		
1	0.43957	- 0.13842	0.30115
2 kN	- 2.13174	0.45869	- 1.67305
3	63.64783	- 5.61513	58.03270
4	10.19532	- 1.65617	8.53915
5 kN-m	-78.19164	9.82650	-68.36514
6	- 4.46240	1.07285	- 3.38954
7	- 0.43957	0.13842	- 0.30115
8 kN	2.13174	-0.45869	1.67305
9	-11.07113	46.49947	35.42834
10	2.92330	-4.29691	-1.37361
11 kN-m	20.61198	-40.88896	-20.27697
12	2.26453	- 0.38074	1.88380
13 kN	47.42330	37.65548	85.07878

$E = 200 \times 10^6$ kPa

$\mu = 0.3$

b = 50 mm ; d = 100 mm

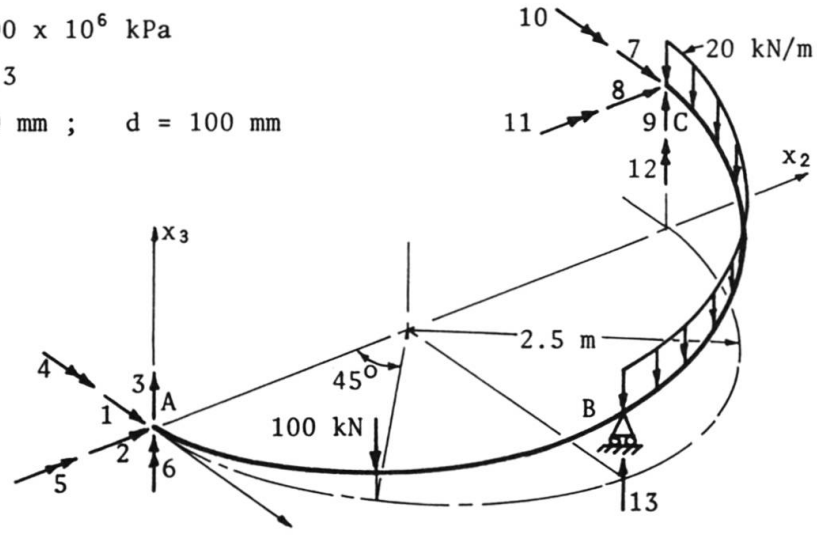

helicoidal member is derived by first evaluating the flexibility matrix at one end which when inverted gives the end stiffness matrix. The Simpson's rule is used to evaluate the integrals associated with the flexibility matrix and equivalent load vector. The effects of axial, bending, shear and torsional deformations are included.

The results from the numerical examples indicate the high degree of accuracy of the proposed numerical method of analysis.

The analysis of helicoidal girders of varying cross-section can be treated quite easily. However, in order to obtain sufficiently accurate solutions more segments to subdivide the girder are generally required.

5. REFERENCES

[1] BERGMAN, V.R.: "Helicoidal Staircases of Reinforced Concrete", Journal ACI, Vol. 28, No. 4, Oct.,1956.

[2] COHEN, J.S.: "Design of Helical Staircases", Concrete and Construction Engineering, Vol. 50, No. 5, London, England, May, 1955.

[3] YOUNG, Y.F. and SCORDELIS, A.C.: "An Analytical and Experimental Study of Helicoidal Girders", Journal of the Structural Division, ASCE, Vol. 84, No. ST5, Proc. Paper 1756, Sept., 1958.

[4] McMANUS, P. et al.: "Horizontally Curved Girders - State-of-the-Art", Journal of the Structural Division, ASCE, Vol. 95, No. ST5, Proc. Paper 6556, May, 1969.

[5] ABDUL-BAKI, A. and SHUKAIR, A.: "Continuous Helicoidal Girders", Journal of the Structural Division, ASCE, Vol. 99, No. ST10, Proc. Paper 10108, Oct., 1973.

[6] DERRON,M. and JIROUSEK,J. : "Elements Spatiaux de Barres Courbes", Publications, International Association for Bridge and Structural Engineering, Zurich, Vol. 36-II, 1976.

[7] HALL, A.S. and WOODHEAD, R.W. : Frame Analysis, John Wiley and Sons, Inc., New York, N.Y., 1967.

[8] GERSTLE, K.H.: Basic Structural Analysis, Prentice-Hall, Inc., Englewood Cliffs, N.J., 1974.